

REENTRANT WETTING TRANSITION OF A ROUGH WALL

Gilberto Giugliarelli

Dipartimento di Fisica and INFN(Gruppo Collegato di Udine, Sezione di Trieste), Università degli Studi di Udine, I-33100 Udine, ITALY

Attilio L. Stella

Istituto Nazionale di Fisica della Materia – Dipartimento di Fisica e Istituto Nazionale di Fisica Nucleare (Sezione di Padova), Università di Padova, I-35131 Padova, ITALY

Abstract

A 2D model describing depinning of an interface from a rough, self-affine substrate, is studied by transfer matrix methods. The phase diagram is determined for several values of the roughness exponent, ζ_S , of the attractive wall. For all $\zeta_S > 0$ the following scenario is observed. In first place, in contrast to the case of a flat wall ($\zeta_S = 0$), for wall attraction energies between zero and a ζ_S -dependent positive value, the substrate is always wet. Furthermore, in a small range of attraction energies, a dewetting transition first occurs as T increases, followed by a wetting one. This unusual reentrance phenomenon seems to be a peculiar feature of self-affine roughness, and does not occur, e. g., for periodically corrugated substrates.

PACS number(s): 68.45.Gd

I. INTRODUCTION

Wetting phenomena occur when, e. g., a layer of liquid phase coexisting with its vapor grows macroscopically over an attractive solid substrate [1]. While wetting in pure systems is relatively well understood by now, the effects of disorder in interfacial phenomena [2–5] pose many challenging issues and are the object of active research. Of particular interest is the effect of geometric surface disorder (roughness) on the location and the nature of the wetting transition. An extensively studied type of roughness, also in view of its experimental realizability [6], is that occurring when the average height fluctuation in a sample of longitudinal linear size L , w_L , scales like $w_L \sim L^{\zeta_S}$. This self-affine scaling disorder is globally characterized by the roughness exponent ζ_S , which can be expected as the only relevant substrate parameter possibly affecting universal features of the wetting transition.

The relevance of ζ_S for both complete and critical wetting transitions has been extensively studied in the last years [7,8]. As far as critical wetting is concerned, a recent study by the present authors [9] has put in evidence the fact that self-affine roughness can produce a change from continuous to first-order transition in systems with short-range forces, when the roughness of the substrate, ζ_S , exceeds the intrinsic roughness of the interface in the bulk, ζ_0 . On the other hand, for $\zeta_S < \zeta_0$, no change is expected in the nature and universality class of the continuous wetting transition, with respect to that on flat substrate.

The possibility that substrate roughness drives a continuous wetting transition first-order has been subsequently discussed in the context of Landau-type mean field approaches [10].

A possible modification of the nature of the wetting transition is not the only effect of self-affine substrate roughness on wetting. As we show here, roughness produces modifications of the phase diagram of the interface, which can be quite dramatic and important in experiments and applications.

In the present paper we study systematically the wetting phase diagram of a generalization [9] of the Chui-Weeks model [11] with a rough attractive boundary in $2D$. By

this study we produce evidence of some remarkable and definitely unusual features of the phase diagram, which, at a qualitative level, should be considered as generic for wetting on self-affine rough substrates. The most notable feature of the phase diagram is a reentrance phenomenon for wetting in the whole range of roughnesses ($0 < \zeta_S < 1$). This reentrance, which implies a dewetting followed by a wetting transition as the temperature is raised, occurs both in regimes when the transitions (both dewetting and wetting) are critical, and when they are first-order.

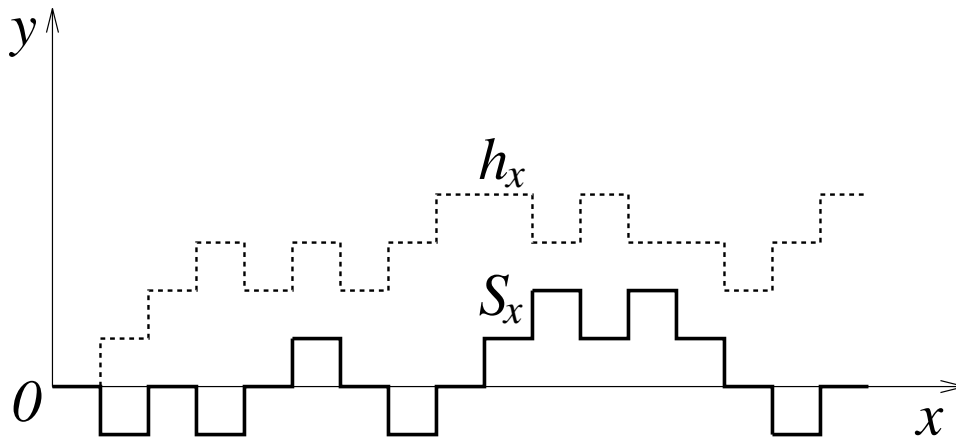


FIG. 1. Example of rough substrate wall (continuous path) and interface configuration (dotted path).

This paper is organized as follows. In the next section we introduce the model and describe the transfer matrix method we apply. In section 3 we discuss how the phase diagram is calculated and illustrate in detail the main results. The last section is devoted to further general considerations and to conclusions.

II. MODEL AND TRANSFER MATRIX

We consider here the same generalization of the Chui-Weeks interfacial model discussed in ref. [9]. Let us denote by x and y the integer coordinates of points on a square lattice.

The interface configurations are self-avoiding paths (partially) directed in the x direction (see Fig. 1). Each interface step parallel to the x axis is located by giving the ordinate $y = h_x$ of its left-hand extremity. In this way the configuration is determined by giving h_x , $\forall x$. We impose the following extra restrictions on the set $\{h_x\}$. First of all $h_x \geq S_x$ where $\{S_x\}$ represents the directed profile of the substrate wall. $\{S_x\}$ are sets of integer ordinates determining the wall configuration with the same conventions applied to $\{h_x\}$. An extra constraint on possible interface configurations is given by $h_{x+1} - h_x = 0, \pm 1$, while for S_x we choose $S_{x+1} - S_x = \pm 1$. We impose such constraints for computational convenience: their removal or modification would not change the main qualitative features of the phase diagram.

The sets $\{S_x\}$ are generated by a random sampling procedure inspired by Mandelbrot [12] and described in Appendix. This procedure produces directed paths in $2D$ obeying the restrictions described above and satisfying the scaling relation

$$\overline{|S_{x+\Delta x} - S_x|} \sim |\Delta x|^{\zeta_s} \quad (1)$$

In the last equation the bar indicates statistical average with respect to the above mentioned sample of $\{S_x\}$. Averages over wall configurations, i. e. over different $\{S_x\}$, will be considered quenched and denoted by overbars below.

The interface Hamiltonian is of the form

$$\mathcal{H} = \sum_x^X [\varepsilon(1 + |z_x - z_{x-1} + s_x|) - u\delta_{z_x,0}] \quad (2)$$

with $z_x = h_x - S_x$ and $s_x = S_x - S_{x-1}$. In eq.(2) ε ($\varepsilon > 0$) is the energy cost of any interface step and $-u$ ($u > 0$) is the energy gain of an interface contact with the attracting wall. The sum in (2) is performed up to X , which represents the length of the interface projection on the x axis. It should be noted that in our model only the horizontal steps of the interface paths in contact with the wall are prized by energies $-u$. This choice is again not mandatory. Different conventions would not change the basic qualitative results.

At a finite temperature T the fugacities $\omega = e^{-\varepsilon/T}$ and $k = e^{u/T}$ are associated with each (horizontal or vertical) step of the path, and to each horizontal step on the wall,

respectively. Consequently, given a wall profile, the partition function associated to all the interface configurations covering a distance X can be written in the form

$$\mathcal{Z}_X = \sum_{\{z_x\}} e^{-\frac{1}{T}[\varepsilon \sum_x^X (1+|z_x-z_{x-1}+s_x|) - u \sum_x^X \delta_{z_x,0}]} = \omega^X \sum_{\{z_x\}} \omega^{n_\perp} k^{n_c} \quad (3)$$

where the sum is done over the ensemble of all the directed paths (determined here by $\{z_x\}$) compatible with the chosen wall. n_\perp and n_c are the number of vertical steps of the interfacial path and the number of horizontal steps on the wall, respectively. Note that the total length of a path is given by $L = X + n_\perp$.

The partition function (3) can be more conveniently expressed in the form

$$\mathcal{Z}_X = \omega^X \sum_{l,z} \left(\prod_{x=1}^X \mathbf{T}_{s_x} \right)_{l,z} \phi_0(z) \quad (4)$$

where the \mathbf{T}_{s_x} are transfer matrices defined as

$$(\mathbf{T}_s)_{m,n} = [\delta_{m,n-s} + \omega(\delta_{m,n-s-1} + \delta_{m,n-s+1})] k^{\delta_{m,0}} \quad (5)$$

with $m, n \geq 0$. The function ϕ_0 in eq. (4) can be used to enforce particular initial conditions for the interface paths; if we choose paths with an extremity on the wall, we put $\phi_0(z) = \delta_{z,0}$.

With the above definitions, a wall profile corresponds to a particular sequence of factors \mathbf{T}_{s_x} in the product of eq.(4). Correspondingly, for asymptotically large systems, the partition function \mathcal{Z}_X can be expressed in terms of the largest Lyapunov eigenvalue λ_{max} as $\mathcal{Z}_X \sim (\omega \lambda_{max})^X$, for $X \rightarrow \infty$, where [13]

$$\lambda_{max} = \lim_{X \rightarrow \infty} \left[\left\| \left(\prod_{x=1}^X \mathbf{T}_{s_x} \right) \vec{\phi}_0 \right\| / \left\| \vec{\phi}_0 \right\| \right]^{\frac{1}{X}} \quad (6)$$

with $\|\vec{\phi}\| = \sum_z \phi(z)$.¹

For walls with some periodic geometry with period X_p the matrix product in (6) can be written as $[\mathcal{T}_{X_p}]^{X/X_p}$ (X assumed an integer multiple of X_p) with $\mathcal{T}_{X_p} = \prod_{x=1}^{X_p} \mathbf{T}_{s_x}$. In this

¹Note that our definition of norm is legitimate because $\phi_0(z)$ and the elements of the \mathbf{T}_{s_x} 's matrices are ≥ 0 .

case the calculation of λ_{max} is equivalent to the calculation of the largest eigenvalue, Λ_{X_p} , of the matrix \mathcal{T}_{X_p} . Consequently, $\lambda_{max} = [\Lambda_{X_p}]^{1/X_p}$.

In numerical calculations it is useful to introduce the normalized vectors $\vec{\psi}_x$ defined by the recursion relation

$$\vec{\psi}_x = \frac{1}{n_x} \mathbf{T}_{s_x} \vec{\psi}_{x-1} \quad (7)$$

with $n_x = \|\mathbf{T}_{s_x} \vec{\psi}_{x-1}\|$ and $\vec{\psi}_0 \equiv \vec{\phi}_0$. It is straightforward to see that the z -th component of the vector $\vec{\psi}_x$ corresponds to the probability that the path at x is at a distance z from the wall [2,8]. This suggests our definition of $\|\vec{\psi}_x\|$. For a given wall profile, the above definitions allow to express the Lyapunov eigenvalue (6) as

$$\lambda_{max} = \lim_{X \rightarrow \infty} \left[\prod_{x=1}^X n_x \right]^{\frac{1}{X}} = \exp \left(\lim_{X \rightarrow \infty} \frac{1}{X} \sum_{x=1}^X \ln n_x \right) \quad (8)$$

The quenched, dimensionless free energy density given by $\lim_{X \rightarrow \infty} -\overline{\ln \mathcal{Z}_X}/X$ can be written in the following form

$$\bar{f} = -\overline{\ln \omega \lambda_{max}} = -\ln \omega - \lim_{X \rightarrow \infty} \frac{1}{X} \overline{\sum_{x=1}^X \ln n_x}. \quad (9)$$

If X is chosen large enough, the average over quenched wall disorder for the second term on the right hand side requires only a rather limited sample of wall configurations. This is due to a self-averaging property of f , which clearly manifests itself in the numerical results.

III. DEPINNING TRANSITION AND PHASE DIAGRAM

In the discussion below we implicitly make u and T dimensionless by dividing them by ε . The wetting transition occurs because, e. g., at a given T , the interface can be bound to the wall of the substrate only for sufficiently high values of u . In the case of ordered flat walls, i. e. $\{S_x = \text{constant} \forall x\}$, the value of u above which the interface is pinned can be easily calculated [14,11,2] to be

$$u_c(T) = T \ln [(1 + 2 \exp(-1/T))/(1 + \exp(-1/T))] \quad (10)$$

with $u_c(0) = 0$. We denote by P_0 the average fraction of interface horizontal steps on the wall,

$$P_0 = \lim_{X \rightarrow \infty} \langle n_c \rangle / X, \quad (11)$$

with brackets indicating canonical thermal average. One can check that P_0 vanishes continuously and linearly when the line $u = u_c(T)$ is approached from above.

When dealing with our random substrates the calculation of P_0 or f for each $\{S_x\}$ can not be done exactly in a semi-infinite geometry, and truncations must be made. To minimize effects of the finite size of the transfer matrices, in our calculations we only considered matrix sizes much larger than the mean square perpendicular width of the self-affine walls. This width can be defined as $\Delta S_{\perp} = (\overline{S^2} - \overline{S}^2)^{1/2} \sim X^{\zeta_s}$, with $\overline{S^2} = (1/X) \sum_x S_x^2$ and $\overline{S} = (1/X) \sum_x S_x$. In practice we used transfer matrices as large as $10^4 \times 10^4$ in the roughest case, corresponding to $\zeta_s = \ln 12 / \ln 32 \simeq 0.717$. With this roughness $X = 10^5$ was reached.

In addition one has to average over different $\{S_x\}$ in order to get $\overline{P_0}$ and \overline{f} . In practice we could sample at most 10 or 15 different $\{S_x\}$ in the most favorable cases, due to the large X 's needed to extract precisely P_0 . Fortunately, as mentioned above, our large X values, of the order of 10^5 , lead to a very high degree of self-averaging in quantities like f and P_0 .

At fixed T , as the transition is approached from above (viz. $u > u_c(T)$) the interface free energy density (9) is negative and increasing, with decreasing u ; at $u = u_c(T)$ it matches the bulk interface free energy density $f_{bulk} = -\ln \omega(1 + 2\omega)$. Thus, it is useful to consider the interface excess free energy density, $\Delta f = \overline{f} - f_{bulk}$, which, by means of eq. (9), can be expressed as

$$\Delta f = -\overline{\ln \lambda_{max}} + \ln(1 + 2\omega) = -\overline{\ln \lambda'_{max}} \quad (12)$$

This last equation defines λ'_{max} as the Lyapunov eigenvalue of transfer matrices defined as $\mathbf{T}'_s = [1/(1 + 2\omega)]\mathbf{T}_s$, which were directly used in our calculations.

Thus the position of the depinning transition corresponds to the vanishing of Δf . Also the interface contact probability can be evaluated using λ'_{max} , taking into account that

$$\overline{P}_0 = k \frac{\partial \Delta f}{\partial k} = \left(\frac{k}{\lambda'_{max}} \right) \overline{\frac{\partial \lambda'_{max}}{\partial k}} = \left(\frac{T}{\lambda'_{max}} \right) \overline{\frac{\partial \lambda'_{max}}{\partial u}} \quad (13)$$

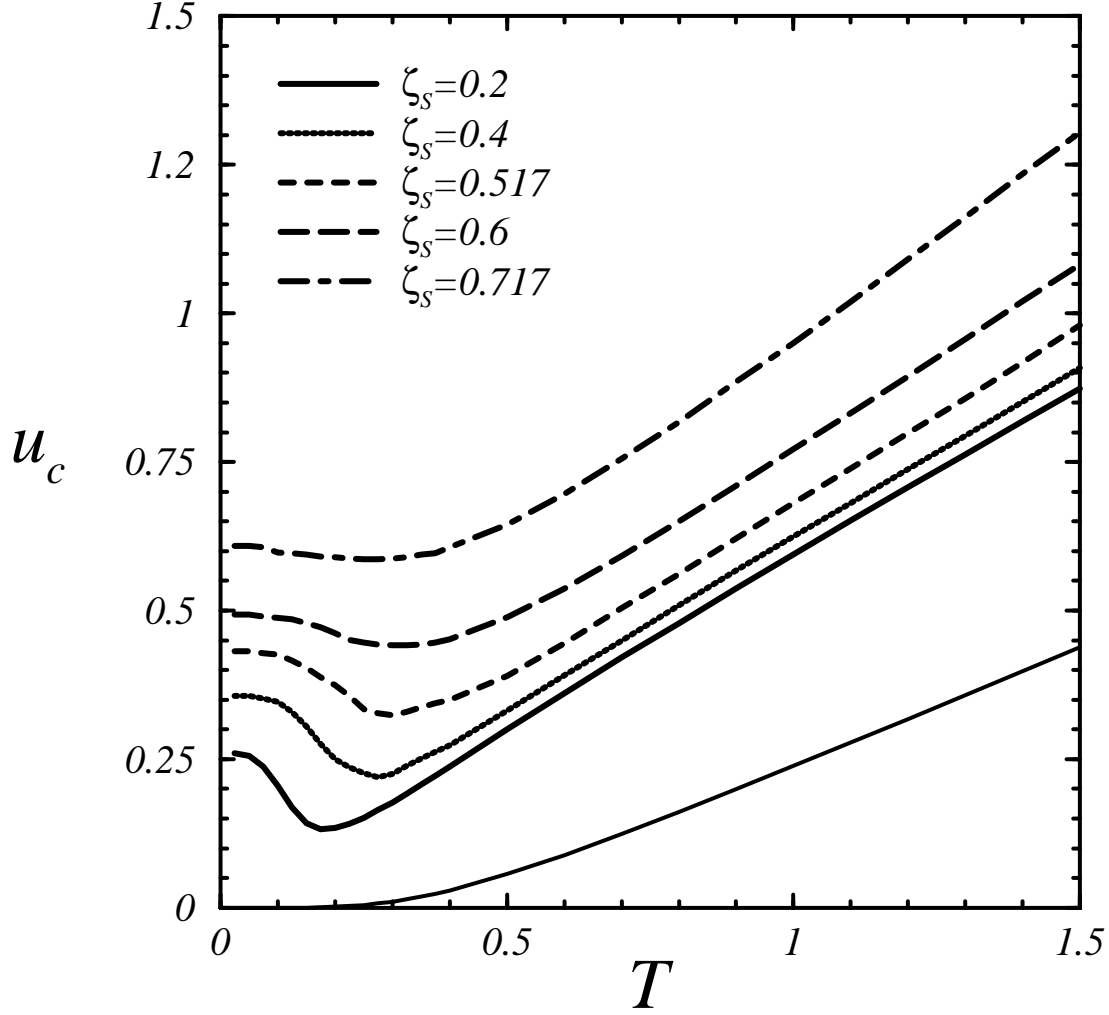


FIG. 2. Interface phase diagram for rough self-affine walls in the T - u plane ($\varepsilon = 1$ is assumed). The curves $u = u_c(T)$ are shown for five different values of the roughness exponent ζ_S . The light continuous line corresponds to $u = u_c(T)$ for a flat wall as given by eq. (10).

The calculation of \overline{P}_0 offers an alternative way of locating dewetting or wetting transitions, by identifying the conditions under which the quantity first becomes zero. A numerical study of how \overline{P}_0 approaches zero can also provide informations on whether these transitions are continuous or discontinuous [9]. We used this criterion, together with an analysis of the way in which Δf vanishes to clarify the first or second order nature of the transitions.

Fig. 2 summarizes the results we have obtained by a systematic calculation of \bar{f} as function of T and u , for 5 different values of the ζ_S . The curves in the figure represent the behavior of u_c versus T . u_c was determined numerically as the value of u below which $|\Delta f| \leq 0.0001$ as u was changed in steps of 0.001. By using the definition of ω and k the $u = u_c(T)$ curves can be converted into the curves $k = k_c(\omega)$. Note that $u_c(0) \neq 0$ implies a power-law divergence of $k_c(\omega)$ for $\omega \rightarrow 0$: $k_c \simeq \omega^{-u_c(0)}$.

Looking at the curves for rough walls in Fig. 2, we note two main differences from the flat case:

- a) It is not possible to pin an interface to a rough wall with a vanishing contact energy. As $T \rightarrow 0$ the minimal contact energy to pin an interface, $u_c(0)$, is finite and increases as the wall roughness, i. e. ζ_S , increases.
- b) For each ζ_S , there is a temperature, $T_R(\zeta_S)$, below which u_c is a decreasing function of T . Note also that for all $\zeta_S < 1$ $u_c(T)$ approaches $u_c(0)$ with zero slope.

A surprising consequence of b) is that if, as in an experiment, we monitor interface behavior at fixed u , by varying T , we have to distinguish among three kinds of regimes:

- I) For $u < u_c(T_R)$ interface pinning is impossible, no matter how low T is. The substrate is wet at all T , and no transitions take place.
- II) for $u > u_c(0)$ as the temperature is increased the interface passes from a pinned to a depinned state at some T_W . Thus, the substrate is partially wet for $T < T_W$ and wet for $T > T_W$, as for smooth walls.
- III) for $u_c(T_R) < u < u_c(0)$, as the temperature is increased, the interface undergoes two transitions: 1) at some temperature $T_D < T_R$ we find an unexpected dewetting: the interface which is depinned for $T < T_D$ becomes pinned at $T = T_D$; 2) at some $T_W > T_R$ a more usual depinning transition follows. Thus, the substrate is wet at very low T , then it dewets, and eventually it wets again at high T .

Unfortunately, a detailed study of the behavior of T_R for ζ_S approaching zero is not feasible due to the necessity of generating extremely long walls in order to distinguish, e. g., $\zeta_S = 0.1$ from $\zeta_S = 0$. However, our results suggest rather clearly that T_R approaches zero for both $\zeta_S \rightarrow 0$ and $\zeta_S \rightarrow 1$. Thus, in these two limits the reentrance disappears.

Another interesting aspect of the phase diagram is that connected to the nature of the transitions involved. The continuous or discontinuous character of the wetting transitions upon varying ζ_S was already discussed in ref. [9] by analyzing the way in which \overline{P}_0 approaches zero for $u \rightarrow u_c(T)$. There we found that when $\zeta_S \lesssim 1/2$ the transition remains second-order and most likely belongs to the same universality class as the flat case, i. e. $\overline{P}_0 \sim (u - u_c)^\psi$, with $\psi = 1$. When ζ_S exceeds $1/2$ there is clear evidence that depinning occurs discontinuously. $\zeta_0 = 1/2$ is the roughness exponent of the interface in the bulk and it makes sense that this is the precise border value of ζ_S separating the two regimes.

A natural question is whether, in the range $u_c(T_R) < u < u_c(0)$, the dewetting transition occurring at low temperature is of the same kind as its wetting counterpart at higher T . Following the lines of ref. [9] we made a systematic study of the dewetting transition for two ζ_S values, respectively below and above $\zeta_S = 1/2$. In the first case ($\zeta_S = 0.4$) we found evidence of a continuous dewetting, while in the latter ($\zeta_S = 0.6$) it appeared discontinuous. Thus, in spite of the fact that the dewetting transition occurs only for some u ranges, and at much lower temperatures, it seems that its character could be the same as that of the corresponding wetting transition. Of course, a more precise definition of the limits within which the above identity of transition orders applies would require an extensive systematic exploration, which is beyond the scope of the present work.

IV. CONCLUSIONS

The results presented in the previous section are somewhat unexpected and are worth discussing further.

FIG. 3. Example of a periodically corrugated wall on a square lattice (heavy line). The wall period is $X_p = 10$. The light straight horizontal line corresponds to the bound interface ground state at $T = 0$ and $u \gtrsim 0$.

The first important fact is that $u_c(0) > 0$ for $\zeta_S > 0$. At $T = 0$, in order to decide whether the interface is pinned or not, we need only to compare the ground state energy in the bulk with the lowest energy of a state in which the interface is bound to the substrate. In the bulk the state of lowest possible energy is clearly given by a straight configuration ($n_\perp = 0$). A bound state will have an energy relative to this unbound ground state equal to $n_\perp - un_c$ (assuming $\varepsilon = 1$). n_\perp and n_c of course depend on the wall configuration to which this bound state refers. Clearly $u_c(0)$ is determined by the condition under which this energy difference between the two states vanishes: $u_c(0) = \lim_{X \rightarrow \infty} n_\perp / n_c$. The fact that bound ground state configurations satisfy this limit condition with $u_c(0) > 0$ is a nontrivial property of self-affine substrates. On a periodically corrugated substrate with average horizontal orientation (like that sketched in Fig. 3) this limit property would not be satisfied. In that case, for u very close to zero, the bound ground state configuration is one in which $n_\perp = 0$, corresponding to a straight interface touching the attractive tips of the periodically corrugated wall (see Fig. 3). Thus, we would have $n_\perp = 0$ and $n_c \neq 0$, and, consequently, $u_c(0) = 0$, like in a flat case. We conclude that a remarkable property of self-affine substrates is that they can support ground state interface configurations with $\lim_{X \rightarrow \infty} n_\perp / n_c > 0$.

Notice further that for a periodically corrugated substrate the reentrance phenomenon with dewetting preceding wetting is not possible, since in that case the curve $u = u_c(T)$ can not be decreasing in the neighborhood of $T = 0$. We verified by explicit calculations that for a wall as in Fig. 3, $u_c(T)$ is in fact never decreasing on the whole T axis.

An even more remarkable property of the self-affine substrate, for which $u_c(0) > 0$ is clearly a necessary but not sufficient condition, is the monotonically decreasing character of the curve $u = u_c(T)$ in the interval $(0, T_R)$. This feature implies that, as soon as $T > 0$, an interface can be more easily bound to the rough substrate. This clearly shows that there is a very nontrivial energy-entropy interplay in the pinning mechanism when self-affine

roughness is involved.

We also compared the nature of dewetting transitions to the corresponding high- T wetting ones. We got only preliminary results on this issue. These results suggest the possibility that, once a first-order character prevails for wetting, the same applies to dewetting as well. This would mean that geometry alone is the crucial factor in determining the nature of transitions on rough substrates.

The model calculations we presented here are of course limited to $2D$ and to strictly short-range forces. An extension in $3D$ is computationally unfeasible, and also the inclusion of long-range potentials would pose serious additional difficulties in our calculations. In $3D$ we expect that the main features of the phase diagram would persist. Of course a major difference in $3D$ would be the character of the transitions. In $3D$ the interface has roughness $\zeta_0 = 0$ in the bulk [2]. Thus, following the conclusions of ref. [9], we should probably expect first-order dewetting and wetting transitions for all $\zeta_S > 0$.

Concerning the effect of long-range forces, which should certainly be included in more realistic calculations to compare with experiments, we can only conjecture that they would not modify the main result obtained here, i. e. the reentrance. However, there is at least one instance, that of interfaces in superconductors [15], in which a short range description is fully adequate.

ACKNOWLEDGMENTS

This work was partially supported by CNR within the CRAY Project of Statistical Mechanics. We are very grateful to T.L. Einstein for a critical reading of the manuscript.

APPENDIX: GENERATING RANDOM SELF-AFFINE PATHS IN $2D$

The procedure we describe here is a random version of a deterministic algorithm by Mandelbrot [12]. Given two even integers, p and q , with $p < q$, the procedure allows us to

construct iteratively a partially directed path with a roughness exponent $\zeta_S = \ln p / \ln q$ and with $X = q^n$ after n iterations.

First we consider a set $\{\vec{\alpha}\}$ of vectors with q components. For each vector $\vec{\alpha}$ in the set $(q + p)/2$ components, chosen at random, are set equal to 1, while the remaining $(q - p)/2$ are put equal to -1 . Once the set $\{\vec{\alpha}\}$ contains a sufficiently large number of such elements, the construction of a wall profile proceeds iteratively. In the first iteration we consider a vector $\vec{\beta}_1$ with q components and, after choosing an element $\vec{\alpha}$ at random in the set $\{\vec{\alpha}\}$, we set $\vec{\beta}_1 = \vec{\alpha}$.

In the second iteration we construct a vector $\vec{\beta}_2$ with q^2 components. Once chosen q vectors $\vec{\alpha}_j$ ($j = 1, 2, \dots, q$) at random in $\{\vec{\alpha}\}$, the components of $\vec{\beta}_2$ are determined according to the rule:

$$\beta_2((j - 1)q + i) = \beta_1(j)\alpha_j(i) \quad (\text{A1})$$

with $i = 1, 2, \dots, q$ and $\alpha_j(i)$ indicating the i -th component of the vector $\vec{\alpha}_j$.

The last equation can obviously be iterated for the construction of vectors $\vec{\beta}_n$ with q^n components:

$$\beta_n((j - 1)q^{n-1} + i) = \beta_{n-1}(j)\alpha_j(i) \quad (\text{A2})$$

with $j = 1, 2, \dots, q^{n-1}$ and $i = 1, 2, \dots, q$.

At any iteration n a directed path defined by the sequence of integers S_x , as explained in section 2, can be obtained from $\vec{\beta}_n$ by

$$S_{x+1} = S_x + \beta_n(x) \quad (\text{A3})$$

where we usually set $S_1 = 0$. Larger n implies a large horizontal size $X = q^n$ of the path. The accuracy of the self-affine average scaling of the paths, as detectable on the basis of eq.(1), increases with increasing n and the number of walls considered. For q ranging between 8 and 32 we have seen that when the longitudinal length of the paths X is of the order of 10^5 the computed roughness exponents of a single generated path coincides with the theoretical $\zeta_S = \ln p / \ln q$ within 1%.

REFERENCES

- [1] For a wide review on wetting phenomena see S. Dietrich, in “*Phase Transitions and Critical Phenomena*”, by C. Domb and J.L. Lebowitz, Vol. 12, (Academic Press, London, 1988).
- [2] G. Forgacs, R. Lipowsky and Th.M. Nieuwenhuizen, in “*Phase Transitions and Critical Phenomena*”, by C. Domb and J.L. Lebowitz, Vol. 14, (Academic Press, London, 1991).
- [3] D.A. Huse and C.L. Henley, *Phys. Rev. Lett.* **54**, 2708 (1985).
- [4] M. Kardar, *Phys. Rev. Lett.* **55**, 2235 (1985); M. Kardar and D.R. Nelson, *Phys. Rev. Lett.* **56**, 472 (1986).
- [5] R. Lipowski and M.E. Fisher, *Phys. Rev. Lett.* **56**, 472 (1986).
- [6] P. Pfeifer, Y.J. Wu, M.W. Cole and J. Krim, *Phys. Rev. Lett.* **62**, 1997 (1989); see also J. Krim, I. Heyvaert, C. Van Haesendonck and Y. Bruynseraede, *Phys. Rev. Lett.* **70**, 57 (1993).
- [7] H. Li and M. Kardar, *Phys. Rev.* **B42**, 6546 (1990); M. Kardar and J.O. Indekeu, *Europhys. Lett.* **12**, 61 (1990).
- [8] G. Giugliarelli and A.L. Stella, *Physica A* **212**, 12 (1994).
- [9] G. Giugliarelli and A.L. Stella, *Phys. Rev. E* **53**, 5035 (1996).
- [10] A.O. Parry, P.S. Swain and J.A. Fox, to be published (1996)
- [11] S.T. Chui and J.D. Weeks, *Phys. Rev.* **B23**, 2438 (1981).
- [12] B.B. Mandelbrot, *Physica Scripta* **32**, 257 (1985).
- [13] A. Crisanti, G. Paladin and A. Vulpiani, in “*Products of Random Matrices in Statistical Physics*”, edited by H.K. Lotsch, Springer Series in Solid State Sciences, Vol.**104** (Springer, Berlin, 1993).

[14] D. Abraham, *Phys. Rev. Lett.* **44**, 1165 (1980).

[15] J.O. Indekeu and J.M.J. van Leeuwen, *Phys. Rev. Lett.* **75**, 1618 (1995).